La Metallurgia Italiana
International Journal of the Italian Association for Metallurgy

Addition of aluminum anodizing waste in different kinds of friction material formulations

P. Jayashree, G. Straffelini

The study focuses on the characterization of aluminum anodizing waste (AAW) in different friction material formulations. AAW was observed to have a dominant presence of hydroxide, sulfate hydrate, and a fraction of alumina. After heat treatment at 400°C for 4.5 hours, the AAW also constituted of AlO_x, obtained from the conversion of hydroxides. The AAW was included in two kinds of friction material compositions – a basic composition (BC) with few constituents, and a commercial composition (CFM), wherein, the AAW was added at 12, 24, and 32 wt.% of variation, and subjected to friction, wear, and emission analysis. The tests were conducted on a pin on disc testing equipment, in mild conditions and at room temperature. The analysis with BC revealed the mild abrasive nature of the AAW, along with acceptable friction, wear, and emission characteristics. With the CFM, the permissible CoF, pin and disc wear, and desirable emission characteristics were observed with 12 wt.% addition of AAW. Higher AAW content led to the degradation of wear and emission characteristics of the CFM specimens. Through this preliminary investigation, the possibility of the recycling/utilization of AAW in friction materials was explored, paving the path for further exploration and feasibility analysis of the inclusion of AAW in braking applications.

KEYWORDS: ALUMINUM, ANODIZING, RECYCLING, INDUSTRIAL WASTE, FRICTION MATERIAL, EMISSIONS, FRICTION, WEAR

INTRODUCTION

The generation of manufacturing by-products or wastes leads to major disposal issues and results in environmental imbalance [1]. Amongst the various aluminum wastes generated (like red mud, salt cakes, dross, and slags [1]), aluminum anodizing waste (AAW) is perhaps one of the most underutilized products [1]–[4]. In their comprehensive review study, Souza et al. [5] have stated that the majority of AAW constitutes ≈80 wt.% of water, along with aluminum hydroxide, calcium/sodium, and aluminum sulfates. Due to similar properties irrespective of the origin, the Al-rich AAW can be utilized as an alternative raw material to produce other materials. A new promising option is to utilize these wastes in friction material compositions. In fact, some studies on the addition of different types of industrial wastes have established precedence for the implementation of other industrial waste alternatives in friction material formulation.

The constituents in a typical friction material can be

P. Jayashree, G. Straffelini
Department of Industrial Engineering,
University of Trento

classified as binders, fillers, reinforcements, and friction modifiers [6]–[8]. Abrasives help in the removal of the pyrolyzed film formed on the counterface surface and impart frictional stability to a wear system. A few examples of abrasives are zirconia, silica, silicon carbide, quartz, alumina, and zirconium silicate [9]–[11] Tomášek et al. [12], Sugözü et al. [13], and Öztürk et al. [10] have shown that the presence of alumina in a non-metallic friction material composition removed negative wear rate and helped elevate and stabilize friction coefficient magnitude. Fan et al. [14] and Boz et al. [15] explained that in semi-metallic friction material, the presence of alumina led to a higher friction coefficient, efficient friction coefficient recovery, and the friction traces were more stable when compared to the wear system without the presence of alumina.

Keeping this in mind, the first part of the current study provides the characterization of AAW, with a detailed and step-by-step analysis of the determination of the appropriate heating cycle and required particle size before adding the AAW in different kinds of friction material formulations. The second part of the study is focused on the friction, emission, and wear behavior of two kinds of friction material formulations with varying AAW content. The first friction material composition was formulated in-house, with only the essential constituents, to highlight the role of the AAW, concerning the friction, wear, and emission characteristics. Considering from the literature, after appropriate heat treatment, the composition of AAW should be like alumina [5]; an ingredient in friction materials that acts as an abrasive. Therefore, two basic formulations were proposed - the first containing AAW, and an alternative to the composition which replaced AAW with alumina particles. Subsequently, a second composition was selected to have a practical application/ approach. A highly optimized friction material formulation, currently being utilized in automotive braking applications was employed with AAW additions at 12, 24, and 32 wt.%. These preliminary tests were mainly aimed at determining the possibility of using AAW in properly developed formulations, without altering its core composition. The tests were carried out using a pin on disc (PoD) apparatus to understand the role of the AAW additions on the wear mechanisms, with the awareness that specific dynamometric bench tests must be carried out in future developments of the research.

MATERIALS AND METHODS

The aluminum anodizing waste (AAW) was provided by Ossicolor SRL, Trento, Italy. The AAW was a dull grey and clumped together. Additionally, the clumps had considerable moisture content in them (close to 75%), originating from the anodizing process.

The first type of friction material composition, in which the AAW was added, was termed 'basic composition' (BC). The BC was developed in-house with the least possible constituents to effectively demonstrate the characteristics of any additives added to the mix. It is assumed that the AAW is like alumina and therefore would behave like an abrasive. On this basis, alumina particles were utilized as abrasives in the reference BC and were later replaced by AAW in the formulation under study. Table 1 shows the composition.

Tab.1 - Characteristic temperatures from thermal analysis of experimental alloys in (°C).

Specimen Code Name	Phenolic Binder	Graphite	Tin Sulfide	Barite & Calcite	Vermiculite	Steel Wool	Iron Powder	Aramid Fibers	Alumina	AAW
BC+Alumina	8	10	10	25	10	5	5	7	20	0
BC+AAW	8	10	10	25	10	5	5	7	0	20

The second friction material composition was an extensively tested and highly optimized commercially employed formulation, containing over 20 ingredients, which are maintained confidential. This composition is termed 'CFM' in this study (Commercial Friction Material). A few of the main constituents and their functions are shown in Table 2 [16]. Four different CFM compositions were tested with varying AAW content; the first was virgin CFM (no AAW addition), followed by 12, 24, and 32 wt.% of AAW in the CFM composition.

Tab.2 - Main constituents of the commercial formulation with their respective function in (wt.%) [16] / Costituenti principali del materiale d'attrito commerciale con la loro funzione tribologica.

Constituents	Function	Content
Phenolic resin	Binder	8
Steel	Reinforcing fibers	30
Vermiculite, others	Fillers	24
Silicon Carbide, Magnesium oxide, Aluminum oxide	Abrasives	25
Graphite, Tin sulfide, Zinc oxide	Lubricants	13

Both friction materials with their respective variations in AAW content were tested in the form of pins. The pins were produced in-house through a standardized procedure [16]. For the sample production with BC, except for the steel wool, the other corresponding constituents listed in Table 1 were measured carefully and mixed in a TURBULA® mixer for 60 mins. After the first round of mixing, the steel wool was then added to the mixture and again mixed for an additional 10 mins. The separate addition and limited time for mixing steel wool ensured that the fibers wouldn't clump together or form agglomerates. On the other hand, with the CFM, no second step in mixing was employed and the mixture with corresponding AAW content was mixed for a continuous 60 mins. The pins were obtained using the hot-pressing technique. The required quantity of powders was 'tap-pressed' in a cylindrical mold made of tool steel and subjected to hot pressing in a BUEHLER® hot mounting press. The production conditions were a compaction pressure of 100 MPa, temperature of 150°C, and holding time of 10 mins. The process was followed by a post-curing method, wherein, the specimens were heated for 4 hours at 200°C in a muffle furnace. The pins were paired with a pearlitic grey cast iron counterface for subsequent wear testing and analysis. The counterface was tested in the form of discs of diameter 60 mm and thickness of 6 mm.

The pins and discs were subjected to dry sliding tests on a pin on disc (PoD) testing apparatus (Ducom Instruments, India). The pins had an average height and diameter of 10 mm. Before the beginning of all tests, the discs were polished thoroughly with a SiC 180 grit abrasive paper and cleaned repeatedly with acetone to remove any dirt, scales, oil, or impurities. Each trial used a fresh new disc. All tests were conducted at room temperature. The testing conditions for all trials were a contact pressure of 1 MPa (79N), and a constant sliding velocity of 1.51 m /s (for a wear track of 48 mm, which amounted to 600 rpm). The testing conditions were chosen to replicate mild braking conditions [17], [18]. Furthermore, mild braking conditions were also employed to observe the characteristics and properties of the deposited secondary contact plateaus, which could have been difficult (with respect to the extension of the secondary contact plateaus) if a 'severe' testing condition was employed. Four trials for each testing condition with varying compositions of AAW in CFM and BC were conducted to obtain repeatability in the results.

Fig. 1 presents the setup of the PoD testing equipment with the particle collection apparatus attachment. The air from the lab (A) was taken in using a fan (B), which was circulated in a High-Efficiency Particulate Air (HEPA) filter (C) to remove dust particles and impurities, leading to the introduction of clean air inside the PoD chamber (D). The air velocity was kept at 11.5 m/s, the magnitude determined from a previous investigation [19]. Before starting any trials, the air cleanliness was always monitored and maintained below 1 #/cm^3.

To obtain the particle number concentration, a TSI® (TSI Incorporated, Shoreview, USA) Optical Particle Sizer Spectrometer (OPS, model 3330) was attached to the enclosed chamber of the PoD testing equipment at site F in Fig. 1. The OPS could measure the total particle number concentration in the size range from 0.3 µm to 10 µm, divided into 16 channels, and with a sampling frequency of 1 Hz [19]. The OPS could record and measure particle concentration up to 3000 particles/cm^3, operating with a self-controlled sampling flow rate of 1 l/min.

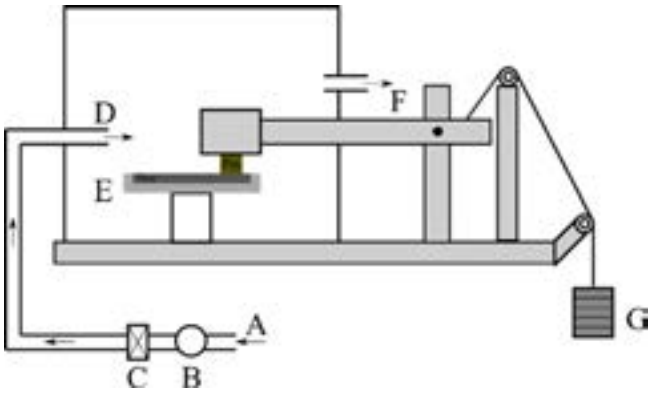

Fig.1 - Testing apparatus setup (A) Ambient air, (B) Fan, (C) HEPA filter, (D) Air introduced in the chamber, (E) Disc/Counterface, (F) Air outlet to the OPS, (G) Weights. / Apparato di prova (A) Ingresso aria esterna; (B) Ventilatore; (C) Filtro HEPA; (D) Aria pulita che entra nella camera; (E) Disco/Antagonista; (F) Uscita dell'aria verso OPS; (G) Pesi.

For both friction material compositions, to obtain proper contact/conformance between the pin and the disc surface, a 'bedding step' was performed for a duration of 30 mins. Following the bedding step, the actual testing duration was 90 continuous minutes to establish desirable conditions for the attainment of a proper friction layer.

The instantaneous magnitude of friction coefficient (CoF) and total particle concentration during the PoD and emission tests were obtained directly from the software connected to the PoD and the OPS equipment respectively. On the other hand, the specific wear coefficient (pin wear) was calculated by weighing the pins before and after each test, using an analytical balance with a precision of 10^{-4} g, and the following equation:

$$K_a = \frac{V}{(F \, x \, d)} \qquad \text{(eq.1)}$$

Where:

V: wear volume loss; F: load applied; d: sliding distance (~8150 m). The disc wear analysis were obtained through a stylus profilometer, acquired perpendicular to the wear track from a transverse profile.

The worn surfaces of the pins and discs and the morphologies of the AAW particles were obtained through SEM (JEOL IT300, JEOL, Japan), attached with Energy Dispersive X-ray Spectroscopy (EDXS; Bruker, USA) system. Further, the AAW particles were also subjected to Thermogravimetric Analysis (TGA, STA 409 PC Luxx®, Germany), X-ray Diffraction (XRD, Italstructures IPD3000 powder diffractometer with an Inel CPS120 detector, Italy), and Fourier Transform Infrared Spectroscopy (FT-IR, Varian Excalibur series 4100, USA) analyses to determine their thermal stability, phase constituents, and composition respectively. The TGA analysis was conducted in the air until 1000°C. From the TGA analysis, the high moisture content in the as received AAW was observed. From the XRD analysis, the AAW was observed to be highly amorphous in nature, thereby, not providing the exact phases [5].

RESULTS

The as-received AAW contains considerable moisture content. Hence, with this high moisture content, the addition of as-received AAW in friction material formulations was not feasible and required heat treatment. Hence, in this study, the as-received AAW was subjected to heat treatment at 400°C for 4.5 hours to remove all the moisture content and potentially convert the Al hydroxide into AlOx as suggested in Ref. 5. After the heat treatment, an apparent change in color was observed; from dark grey to light orange, signifying a change in the constituent

phase of the AAW [5].

To understand the morphology of the AAW, the heat-treated powder was subjected to SEM and point EDXS analysis. Fig. 2 (a) represents the low magnification SEM image. Two distinctive shapes can be observed – well-rounded ones and flat-faced sharp-edged. The sharp edges and flat faces could be attributed to the crushing of the AAW clumps and then to their brittleness. The EDXS analysis showed that the particles mainly contain Al (43%) and O (45%), and constituents like Ca and Sn that can be considered minor constituents.

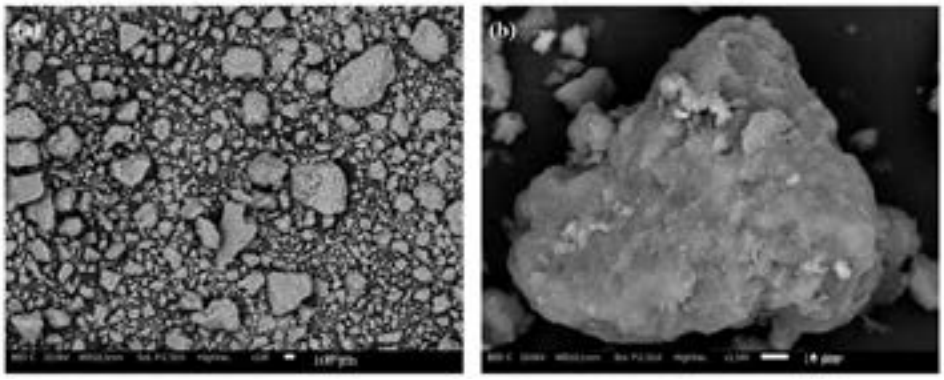

Fig.2 - (a) Low magnification; (b) High magnification image of one AAW particle treated at 400°C for 4.5 hours. Immagine SEM delle particelle trattate a 400°C per 4.5 ore. / (a) Basso ingrandimento; (b) Alto ingrandimento.

Next, to select the best particle size, the heat-treated AAW was sieved to two particle sizes - <180 μm and <90 μm. Both particle size samples were added separately to the CFM composition and mixed for 1 hour. It was observed that the mixture containing <180 μm particles did not mix well with the CFM and would settle at the bottom of the mixing bottle. On the other hand, the mixture containing <90 μm had undergone uniform mixing with no settlement at the bottom. Hence, for the friction and emission analysis, AAW heat-treated at 400°C for 4.5 hours and sieved to <90 μm were added to the BC and CFM (at 12, 24, and 32 wt.%) compositions.

A slight decrease in the density of the produced materials is observed with the replacement of alumina by AAW. Nevertheless, the pin density for both BC pins (with alumina and AAW) is high, in the range of 2.26-2.5 g/cm^3. With the CFM, a steady decrease in the pin density was observed with the increase in the AAW content. The CFM has a density of 2.26 g/cm^3, and the least density was seen for CFM with 32 wt.% AAW addition, which was close to 1.87 g/cm^3.

Table 3 compares the steady state CoF, average (steady state) particle concentration, and pin and disc wear of BC with alumina and AAW. With respect to BC containing AAW, we see similar CoF and pin wear, and a slight decrease in average (steady state) particle concentration when compared to the alumina containing BC. On the other hand, the disc wear for BC AAW is lower than BC alumina, even if in both cases, the wear can be classified as 'very mild'.

Tab.3 - Friction, wear, and emission characteristics of BC containing alumina and AAW. / Attrito, usura ed emissioni delle formulazioni BC contenenti allumina e AAWW.

Specimens	Steady State Friction Coefficient	Specific Wear Coefficient of Pin (m^2/N)	Specific Wear Coefficient of Disc (m^2/N)	Average Particle Concentration (#/cm^3)
BC + Alumina	0.44±0.02	(1.47±0.029)10^{-14}	(0.38±0.007)10^{-14}	402±12
BC + AAW	0.45±0.01	(1.43±0.36)10^{-14}	(0.047±0.005)10^{-14}	363±183

Table 4 shows the steady state coefficients of friction (CoF) magnitudes of CFM and with AAW additions. The CoF magnitude is observed to slightly increase with the addition of 12 and 24 wt.% of AAW. On the other hand, a significant increase of steady state CoF is observed at 32% of AAW addition. For the average (steady state) particle concentration, the magnitude steadily increases with an increase in the AAW content. In the case of pin wear, like the average particle concentration, a steady increase in pin wear is observed with an increase in AAW content. All the pin wear magnitude is categorized in the 'mild to severe' wear regime (wear above $2x10^{-14}$ m^2/N and below 10^{-13} m^2/N). A broadly similar trend was observed with the disc wear. In particular, the disc wear for 24 and 32% of AAW addition in CFM are similar to each other

Tab.4 - Friction, wear, and emission characteristics of BC containing alumina and AAW. / Attrito, usura ed emissioni delle formulazioni BC contenenti allumina e AAWW.

Specimens	Steady State Friction Coefficient	Specific Wear Coefficient of Pin (m^2/N)	Specific Wear Coefficient of Disc (m^2/N)	Average Particle Concentration ($\#/cm^3$)
CFM	0.43±0.02	$(3.41±0.29)10^{-14}$	$(3.61±0.50)10^{-14}$	435±148
CFM + 12% AAW	0.47±0.04	$(3.98±0.16)10^{-14}$	$(2.52±0.34)10^{-14}$	538±379
CFM + 24% AAW	0.48±0.01	$(5.09±0.23)10^{-14}$	$(4.95±0.71)10^{-14}$	749±332
CFM + 32% AAW	0.61±0.02	$(7.2±0.64)10^{-14}$	$(4.87±0.95)10^{-14}$	1039±273

Fig. 3 shows the worn pin surfaces of BC alumina and BC AAW. It is widely known that the primary contact plateaus like steel fibers assist in and compact the wear debris produced during sliding, which is known as the secondary plateaus. In Fig. 3 (a), the surface is covered by bright white regions shown by red dots. They are steel fibers. Additionally, the presence of compacted and well-spread light grey regions can be observed. These regions are the secondary plateaus. From the EDXS analysis, we can see that these regions are made of Fe and O (overlap of Fe and O maps), inferring Fe oxides [6], [18]. The observations with the BC pin containing AAW (Fig. 4 (b)) are similar to the BC pin containing alumina (Fig. 3 (a)), in terms of the primary and secondary plateau characteristics.

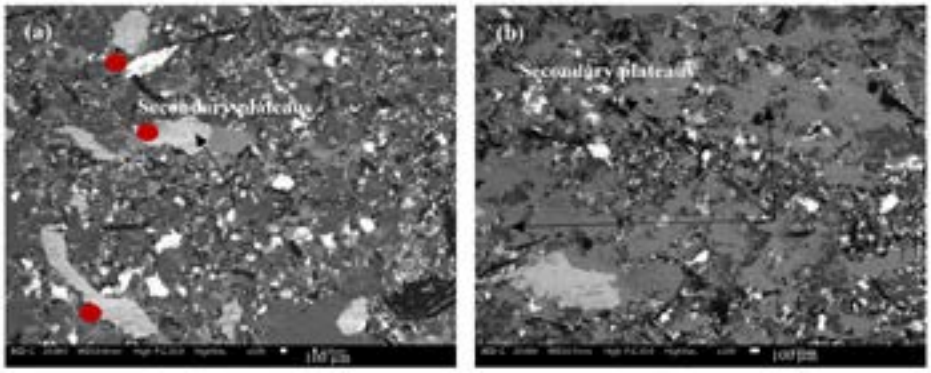

Fig.3 - Worn pin surfaces (a) BC with alumina; (b) BC with AAW / Superfici usurate dei materiali d'attrito. (a) BC con allumina; (b) BC con AAW.

To ascertain the composition, point EDXS analyses were conducted on six different sites on the secondary plateaus for both BC compositions. The results are shown in Table 5. The primary constituent of the secondary plateaus is Fe oxides. The Fe oxide is accompanied by other minor constituents like Al, Ba, Sn, Mg, and Ca. It should be noted that the Fe content in BC AAW is slightly lesser than the Fe content in the secondary plateaus of BC alumina.

Fig. 4 shows the worn CFM pin surface. Like the observation with the BC samples, the worn surface constitutes bright regions (steel fibers), smooth and well-compacted light grey regions (secondary plateaus), and black regions (graphite). The secondary plateaus are not only deposited in the vicinity of the primary plateaus but are also present throughout the worn surface. The secondary plateaus are made of Fe oxides [16].

Tab.5 - Point/object analysis of the secondary plateaus deposited on the worn BC pin surface with alumina and AAW. / Analisi puntuale mediante EDXS dei plateaux secondari presenti sulle superfici di usura dei materiali BC.

Element	BC+ alumina Wt. %	BC+AAW Wt. %
Iron	43±5	36±11
Oxygen	34±1	37±4
Silicon	1±0.4	2±0
Tin	4±1	8±6
Barium	5±1.5	5±0
Magnesium	2±1	2±0.1
Calcium	3±1	2.5±0.4
Aluminum	6±1.5	4±1
Sulfur	2±1	3.5±1.6

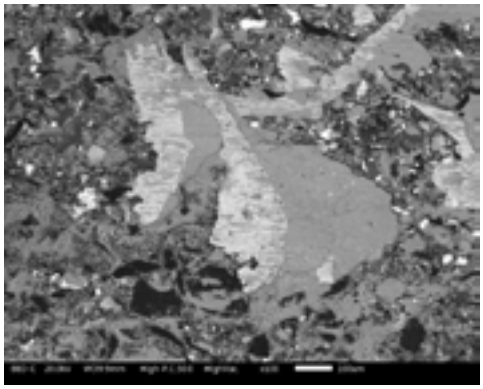

Fig.4 - SEM BSE image of the worn CFM pin surface. / Osservazione SEM (BSE) della superficie di usura del materiale CFM.

Similar to Table 5, Table 6 compiles the point EDXS analysis of secondary plateaus on CFM specimens. Like the secondary plateaus of the BC, the presence of Fe and O suggests Fe oxides, as known from previous studies [10], [17]. Additionally, the presence of Al is observed to naturally increase with the increase in AAW content. The secondary plateaus constitute other minor constituents like Zn, Si, Sn, and Mg.

To further understand the extension of the presence of Al particles on the secondary plateaus of BC and CFM with their respective AAW additions, a basic estimation of the area was conducted on the worn surfaces using the ImageJ open-source software with reference to the EDXS maps of Al. The obtained data are shown in Table 7. In the case of BC, the Al coverage for BC Alumina and BC AAW are quite similar. For CFM, an obvious increase in the Al coverage is seen with the increase in the AAW content. The Al coverage increases from 11% (CFM) to 40% (32% AAW).

As an example, Fig. 5 shows the worn disc profiles paired with BC containing alumina and AAW. In the case of BC alumina, Fig. 5 (a), deep grooves/scratches can be easily observed in the direction of sliding. On the other hand,

for the BC AAW, Fig. 5 (b), though the surface presents scratches, they are not as deep or severe as the ones observed with BC alumina.

For CFM and with AAW variations, the worn surface characteristics were similar to Fig. 5. However, the intensity of scratches/abrasions on the disc surface was observed to increase with the AAW content.

Tab.6 - Point/object analysis of the secondary plateaus deposited on the worn CFM pin surface with varying AAW content. / Analisi puntuale mediante EDXS dei plateaux secondari presenti sulle superfici di usura dei materiali CFM.

Element	CFM Wt. %	CFM + 12% AAW Wt. %	CFM + 24% AAW Wt. %	CFM + 32% AAW Wt. %
Iron	64±4	59±3	60±4	59±4
Oxygen	28±4	25±4	27±1	26±3
Silicon	1.2±0.1	1.8±0.3	1.4±0.5	1±0.06
Tin	1.7±0.3	2±0.2	1.2±0.2	2±0.2
Chromium	0.5±0.2	0.7±0.2	0.4±0.06	0.5±0.2
Magnesium	1.4±0.2	2±0.1	1.5±0.5	1.2±0.1
Calcium	0±0	0±0	1±0.5	0.8±0.1
Aluminum	1±0.1	4±0	5±1	6±0.6
Sulfur	1±0.1	1.7±0.1	1.2±0.15	2±0.3
Zinc	2±0.2	3±0.6	1.8±0.4	2±0.2
Manganese	0.5±0.04	0±0	0.4±0.04	0.4±0

Tab.7 - Area estimation of Al coverage in the secondary plateaus, obtained from the EDXS maps (from ImageJ analysis software). / Estensione delle zone di Al nei plateaux secondari, ottenuta dalla mappe EDXS (usando il software ImageJ).

Specimens	Area Estimation of Al Coverage (%)
BC + Alumina	21±4
BC + AAW	19±3
CFM	11±2
CFM + 12% AAW	21±4
CFM + 24% AAW	27±2
CFM + 32% AAW	40±3

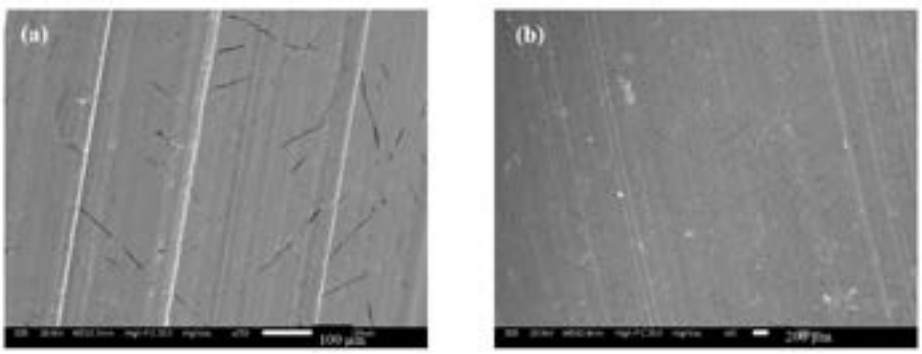

Fig.5 - Worn disc surfaces (a) BC with alumina; (b) BC with AAW / Superfici di usura dei dischi. (b) BC contenente allumina; (b) BC contenente AAW.

DISCUSSION

The AAW analyzed in this study was received without any pre-treatment, resulting in high moisture content due to the aluminum anodizing process. During the heat treatment at 400°C for 4.5 hours, a change in the color characteristics of the AAW was observed – from dull grey to light orange, signifying phase change. [5]. In a previous investigation, it has been also shown that the as received powder is amorphous and the heat treatment induces a partial conversion of aluminum hydroxide into AlOx [22]. The addition of powder with size <90 μm resulted in uniform mixing of the AAW in the CFM and BC composition. Nevertheless, the addition of smaller AAW particles led to its subsequent large volume addition in the mix, resulting in a reduction of the pin density. This explains the lowering density with an increase in the AAW content in CFM composition in Table 5. When compared to the BC composition, the CFM composition inherently has low density, which is further reduced at high AAW additions (especially at 32 wt.%).

The tests with the basic composition (BC) were intended to understand the AAW characteristics from the friction, wear, and emission studies. As observed, the AAW constituted of Al-oxide and hence was perceived as abrasive and compared to a BC composition containing conventional alumina in it. Kim et al. [20] investigated the role of different abrasives and the CoF was in the order of silicon carbide> zircon > quartz > magnesia. Fan et al. [14] investigated the role of alumina particles and when comparing the CoFs, it was inferred that the abrasion properties of alumina particles were intermediate [12]. The tests with the BC enforced this observation, showing that the AAW behaves as an abrasive, as it had similar friction and wear behavior when compared to the BC alumina specimens. However, the abrasive nature and characteristics of AAW were milder than conventional alumina. The AAW were found in the secondary plateaus, which led to the counterface abrasion. This is validated by the softer scratches on the counterface surface, leading to lower Fe presence in the secondary plateaus on the worn BC AAW surface and lower disc wear. As mentioned, the wear of the BC friction material was mild, and that of the counterface disc was very mild. Therefore, it is expected that the emissions of airborne particles are low as well. From previous observations [19], [21], it was shown that the particle concentration below 500 #/cm^3 is considered to be a low value. In the case of BC with AAW, the particle concentration was well below 500 #/cm^3, showing desirable emission characteristics, along with permissible CoF, and pin and disc wear.

As previously mentioned, the CFM utilized in this study is a highly optimized friction material composition. Due to its efficient combination of constituents, any change in its composition would immediately affect its wear and emission characteristics. Since it is already known from the BC tests that the AAW is a mild abrasive, it is then expected that any variation in the CFM properties would directly be attributed to the AAW addition. As a matter of fact, an increase in CoF is observed with an increase in AAW content. To better clarify this point, Fig. 6 represents the relationship between the average CoF with the Al area coverage on the worn pin surfaces of the CFM specimens. It can be seen that as the Al area coverage increases, so does the average CoF. Essentially, the Al particles enter the secondary plateaus and act as an abrasive, thereby, increasing the CoF. The abrasive character of AAW was further enforced with high disc wear at elevated AAW content.

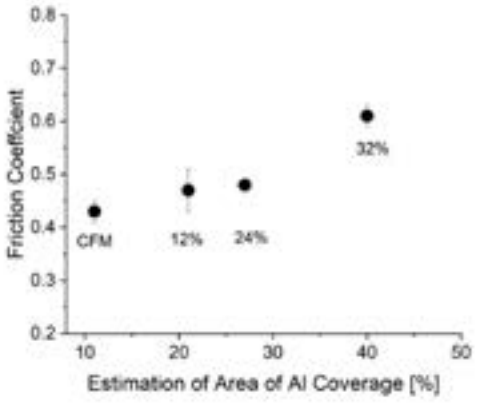

Fig.6 - Comparison of average CoF with the average estimation of Al area coverage for CFM and its AAW variations. / Dipendenza sperimentale del coefficiente d'attrito con l'estensione dei plateaux secondari contenenti particelle di AAW.

Straffelini and Gialanella [21], and Nogueira et al. [19] have presented a concrete proportional relationship between the average CoF and average particle concentration of a wear system. Similar observations were also recorded in this study. For the CFM specimens, an increase in CoF observed an increase in emissions. Hence, the 32% addition of AAW observed the highest emissions (with the highest CoF) and the 12% AAW addition had comparatively low emissions (with the lowest CoF) in all AAW containing CFM specimens, as seen in Fig. 7.

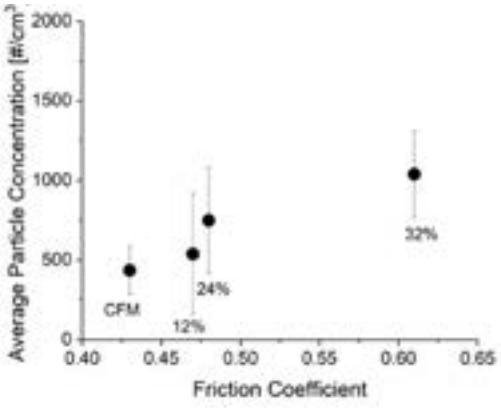

Fig.7 - Comparison of average particle concentration with the average CoF for CFM and its AAW variations. / Dipendenza sperimentale della composizione media di polveri sottili emesse con il coefficiente d'attrito.

As the AAW is a mild abrasive, at 12 wt.% addition in CFM, lower wear, optimum CoF, and permissible average particle concentration were observed. The CFM composition already constitutes abrasives and with the addition of 12 wt.% of AAW, the wear and emission characteristics of the CFM were not changed significantly. Hence, the 12 wt.% addition of CFM is the ideal addition, compared to the higher AAW addition which varied the CFM characteristics drastically.

Through the initial analysis conducted on the one-of-a-kind addition of aluminum anodizing waste (AAW) in different friction material formulations, the positive effects of the addition of AAW were observed, the addition being limited to 12 wt. %. The future work of this study will be focused on specific dynamometric testing to appropriately establish the behavior of the friction materials at effective braking conditions. After a comprehensive analysis and conducting a feasibility check, a modified version of CFM could be produced, wherein, an abrasive fraction could be removed and replaced by AAW, while still maintaining its highly optimized composition and well-balanced wear and emission characteristics.

CONCLUSIONS

In a novel attempt to effectively recycle aluminum anodizing waste (AAW), this study focuses on the feasibility of its utilization in friction material compositions.

- The as-received AAW was characterized to understand its thermal stability and composition. The FT-IR analysis revealed that the hydroxide and sulfate hydrate curves shrunk with an increase in temperature. Additionally, all the samples at different temperature treatments recorded the presence of alumina. As the as-received AAW had a high moisture content, the AAW was subjected to heat treatment at 400°C for 4.5 hours, as the temperature was apt to convert hydroxide into AlO_x, which was witnessed by the change in the AAW color from light grey to orange, and by SEM analysis. Further, the particle size was maintained at <90 μm for homogeneous distribution of the AAW in the friction material composition.
- The wear and emission analysis were conducted by adding the heat-treated and sieved AAW to the basic composition (BC) and commercial friction material (CFM) composition. With the BC, the AAW was compared with conventional alumina. The CoF and pin wear were similar. The emissions were slightly reduced, and the disc wear was significantly lower when compared to BC alumina. These observations highlighted the role of AAW as a mild abrasive, further validated by the low presence of Fe in the secondary plateaus.

- With the CFM, the higher the AAW content, the higher the CoF, pin and disc wear, and emissions. Essentially, the AAW enters the secondary plateaus and causes abrasive wear on the counterface, resulting in an increase in disc wear. The higher CoF is attributed to the abrasive action of the AAW, which in turn, resulted in higher emissions at elevated AAW content.
- The addition of 12 wt.% of AAW in CFM produced comparable CoF, pin wear, and emissions to virgin CFM. Along with the already present abrasives in the CFM composition, the 12 wt.% addition of AAW worked extremely well without altering the CFM properties significantly. Hence, through this analysis of the suitability of the addition of AAW in friction material formulation, the feasibility of the waste addition was clearly observed.

ACKNOWLEDGMENTS

The authors would like to thank Dr. Roberto Masciocchi of Ossicolor SRL., Trento, Italy, for providing the raw material and for the helpful discussions.

REFERENCES

[1] A. Erdoğan, M. S. Gök, V. Koç, and A. Günen, "Friction and wear behavior of epoxy composite filled with industrial wastes," Journal of Cleaner Production, vol. 237, Nov. 2019, doi: 10.1016/j.jclepro.2019.07.063.

[2] L. F. Xavier and P. Suresh, "Wear Behavior of Aluminium Metal Matrix Composite Prepared from Industrial Waste," Scientific World Journal, vol. 2016, 2016, doi: 10.1155/2016/6538345.

[3] R. Galindo, I. Padilla, O. Rodríguez, R. Sánchez-Hernández, S. López-Andrés, and A. López-Delgado, "Characterization of Solid Wastes from Aluminum Tertiary Sector: The Current State of Spanish Industry," Journal of Minerals and Materials Characterization and Engineering, vol. 03, no. 02, pp. 55–64, 2015, doi: 10.4236/jmmce.2015.32008.

[4] H. Kumar, R. Prasad, P. Kumar, S. P. Tewari, and J. K. Singh, "Mechanical and tribological characterization of industrial wastes reinforced aluminum alloy composites fabricated via friction stir processing," Journal of Alloys and Compounds, vol. 831, Aug. 2020, doi: 10.1016/j.jallcom.2020.154832.

[5] M. T. Souza, L. Simão, O. R. K. Montedo, F. Raupp Pereira, and A. P. N. de Oliveira, "Aluminum anodizing waste and its uses: An overview of potential applications and market opportunities," Waste Management, vol. 84. Elsevier Ltd, pp. 286–301, Feb. 01, 2019. doi: 10.1016/j.wasman.2018.12.003.

[6] M. Leonardi, C. Menapace, V. Matějka, S. Gialanella, and G. Straffelini, "Pin-on-disc investigation on copper-free friction materials dry sliding against cast iron," Tribology International, vol. 119, no. October 2017, pp. 73–81, 2018, doi: 10.1016/j.triboint.2017.10.037.

[7] J. Kukutschová et al., "Wear performance and wear debris of semimetallic automotive brake materials," Wear, vol. 268, no. 1, pp. 86–93, 2010, doi: 10.1016/j.wear.2009.06.039.

[8] G. Straffelini and L. Maines, "The relationship between wear of semimetallic friction materials and pearlitic cast iron in dry sliding," Wear, vol. 307, no. 1–2, pp. 75–80, 2013, doi: 10.1016/j.wear.2013.08.020.

[9] B. Pérez and J. Echeberria, "Influence of abrasives and graphite on processing and properties of sintered metallic friction materials," Heliyon, vol. 5, no. 8, 2019, doi: 10.1016/j.heliyon.2019.e02311.

[10] B. Öztürk, S. Ö. Ztürk, and A. A. Adigüzel, "Effect of type and relative amount of solid lubricants and abrasives on the tribological properties of brake friction materials," Tribology Transactions, vol. 56, no. 3, pp. 428–441, 2013, doi: 10.1080/10402004.2012.758333.

[11] V. Tomášek, G. Kratošová, R. Yun, Y. Fan, and Y. Lu, "Effects of alumina in nonmetallic brake friction materials on friction performance," Journal of Materials Science, vol. 44, no. 1, pp. 266–273, 2009, doi: 10.1007/s10853-008-3041-z.

[12] V. Tomášek, G. Kratošová, R. Yun, Y. Fan, and Y. Lu, "Effects of alumina in nonmetallic brake friction materials on friction performance," Journal of Materials Science, vol. 44, no. 1, pp. 266–273, Jan. 2009, doi: 10.1007/s10853-008-3041-z.

[13] B. Sugözü, B. Dağhan, and A. Akdemir, "Effect of the size on the friction characteristics of brake friction materials: a case study with Al2O3," Industrial Lubrication and Tribology, vol. 70, no. 6, pp. 1020–1024, Aug. 2018, doi: 10.1108/ILT-02-2017-0035.

[14] Y. Fan, V. Matějka, G. Kratošová, and Y. Lu, "Role of al2o3 in semi-metallic friction materials and its effects on friction and wear performance," Tribology Transactions, vol. 51, no. 6, pp. 771–778, 2008, doi: 10.1080/10402000802011760.

[15] M. Boz and A. Kurt, "The effect of Al2O3 on the friction performance of automotive brake friction materials," Tribology International, vol. 40, no. 7, pp. 1161–1169, 2007, doi: 10.1016/j.triboint.2006.12.004.

[16] V. Matějka, M. Leonardi, P. Praus, G. Straffelini, and S. Gialanella, "The Role of Graphitic Carbon Nitride in the Formulation of Copper-Free Friction Composites Designed for Automotive Brake Pads," Metals (Basel), vol. 12, no. 1, p. 123, Jan. 2022, doi: 10.3390/met12010123.

[17] M. Leonardi, M. Alemani, G. Straffelini, and S. Gialanella, "A pin-on-disc study on the dry sliding behavior of a Cu-free friction material containing different types of natural graphite," Wear, vol. 442–443, no. November 2019, p. 203157, 2020, doi: 10.1016/j.wear.2019.203157.

[18] C. Menapace, M. Leonardi, V. Matějka, S. Gialanella, and G. Straffelini, "Dry sliding behavior and friction layer formation in copper-free barite containing friction materials," Wear, vol. 398–399, no. July 2017, pp. 191–200, 2018, doi: 10.1016/j.wear.2017.12.008.
[19] A. P. G. Nogueira, D. Carlevaris, C. Menapace, and G. Straffelini, "Tribological and emission behavior of novel friction materials," Atmosphere (Basel), vol. 11, no. 10, 2020, doi: 10.3390/atmos11101050.
[20] S. S. Kim, H. J. Hwang, M. W. Shin, and H. Jang, "Friction and vibration of automotive brake pads containing different abrasive particles," Wear, vol. 271, no. 7–8, pp. 1194–1202, 2011, doi: 10.1016/j.wear.2011.05.037.
[21] G. Straffelini and S. Gialanella, "Airborne particulate matter from brake systems: An assessment of the relevant tribological formation mechanisms," Wear, vol. 478–479, no. January, 2021, doi: 10.1016/j.wear.2021.203883.
[22] P. Jahashree and G. Straffelini, "The influence of the addition of aluminum anodizing waste on the friction and emission behavior of different kinds of friction material formulations", Tribology International, vol. 173, 2022, doi: 10.1016/j.triboint.2022.107676.

Aggiunta di scarti di anodizzazione dell'alluminio in diverse formulazioni di materiali di attrito

Lo studio si concentra sulla caratterizzazione e l'utilizzo di scarti di anodizzazione dell'alluminio (AAW) nella formulazione dei materiali di attrito. Gli scarti hanno un contenuto dominante di idrossido e solfato di alluminio. Dopo trattamento termico a 400°C per 4.5 ore, l'AAW è costituito anche da AlO_x, ottenuto dalla conversione degli idrossidi. L'AAW è stato quindi aggiunto in due tipi di composizioni di materiali di attrito: una composizione di base (BC) con pochi costituenti e una composizione commerciale (CFM), in cui l'AAW è stato aggiunto al 12, 24 e 32% in peso. I materiali prodotti sono stati quindi sottoposti a prove di strisciamento a secco, con l'obiettivo di studiarne il comportamento triboilogico durante frenata automobilistica in condizioni moderate. I test sono stati condotti su un'apparecchiatura "perno contro disco" (PoD), in condizioni di test moderate, a temperatura ambiente, misurando il coefficiente di attrito, l'usura dei campioni e dei dischi e le emissioni in ambiente di polveri sottili. Lo studio della composizione base ha rivelato la natura leggermente abrasiva dell'AAW, insieme a caratteristiche accettabili di attrito, usura ed emissione. Questo risultato è stato sostanzialmente confermato nelle prove con la composizione commerciale. In questo caso è stata anche studiato il limite massimo di possibile aggiunta delle polveri AAW, senza degradare le prestazioni tribologiche. Un'aggiunta del 12% in peso di AAW si è rivelata ottimale. In questa indagine preliminare, è stata esplorata la possibilità del riciclaggio/utilizzo dell'AAW in materiali d'attrito, aprendo la strada a ulteriori analisi di fattibilità dell'inclusione dell'AAW nei sistemi di frenata.

PAROLE CHIAVE: ALLUMINIO, ANODIZZAZIONE, RICICLAGGIO, RIFIUTI INDUSTRIALI, MATERIALE DI ATTRITO, EMISSIONI, ATTRITO, USURA

TORNA ALL'INDICE >